Published in final edited form as:
Nature. 2009 September 3; 461(7260): 109–113. doi:10.1038/nature08268.

Antioxidant and Oncogene Rescue of Metabolic Defects Caused by Loss of Matrix Attachment

Zachary T. Schafer[1,4], **Alexandra R. Grassian**[1,†], **Loling Song**[1,†], **Zhenyang Jiang**[1], **Zachary Gerhart-Hines**[2,3], **Hanna Y. Irie**[1], **Sizhen Gao**[1], **Pere Puigserver**[1,2], and **Joan S. Brugge**[1,*]

[1]Department of Cell Biology, Harvard Medical School, Boston, MA, 02115

[2]Department of Cancer Biology, Dana-Farber Cancer Institute, Boston, MA, 02115

[3]Department of Cell Biology, Johns Hopkins University School of Medicine, Baltimore, MD, 21205

Abstract

Normal epithelial cells require matrix attachment for survival and the ability of tumour cells to survive outside their natural extracellular matrix (ECM) niches is dependent on acquisition of anchorage independence1. While apoptosis is the most rapid mechanism for eliminating cells lacking appropriate ECM attachment2, recent reports suggest that non-apoptotic death processes prevent survival when apoptosis is inhibited in matrix-deprived cells3,4. Here we demonstrate that detachment of mammary epithelial cells from ECM causes an ATP deficiency due to loss of glucose transport. Overexpression of ErbB2 rescues the ATP deficiency by restoring glucose uptake through stabilization of EGFR and PI(3)K activation and this rescue is dependent on glucose-stimulated flux through the antioxidant-generating pentose phosphate pathway (PPP). Interestingly, we found that the ATP deficiency could be rescued by antioxidant treatment without rescue of glucose uptake. This rescue was found to be dependent on stimulation of fatty acid oxidation (FAO), which is inhibited by detachment-induced reactive oxygen species (ROS). The significance of these findings was supported by evidence of an elevation in ROS in matrix-deprived cells in the luminal space of mammary acini and that antioxidants facilitate the survival of these cells and enhance anchorage-independent colony formation. These results reveal both the importance of matrix attachment in regulating metabolic activity and an unanticipated mechanism for cell survival in altered matrix environments through antioxidant restoration of ATP generation.

Epithelial cells are dependent on interactions with specific extracellular matrix (ECM) components for survival, proliferation, and differentiation functions[5]. Loss of matrix attachment of cultured epithelial cells activates a caspase-mediated apoptotic program known as anoikis2. In glandular cancers, like breast cancer, tumour cells are displaced from their

*To whom correspondence should be addressed: Department of Cell Biology, Harvard Medical School, 240 Longwood Avenue, Boston, MA 02115, Phone: 617-432-3974, Fax: 617-432-3969, joan_brugge@hms.harvard.edu.
[4]Present address: Department of Biological Sciences, University of Notre Dame, Notre Dame, IN 46556
†These authors contributed equally to this work.

Supplementary information is linked to the online version of the paper at www.nature.com/nature. A figure summarising the main result of this paper (Supplementary Fig. 1) is included in the supplementary information.

Author Contributions

Z.T.S. and J.S.B. were responsible for the overall study design. Z.T.S., A.R.G., H.Y.I., and S.G. conducted experiments. L.S. and Z.J. conducted the experiments measuring native fluorescence of NAD(P)H in 3D cell culture. Z.G.-H. and P.P. designed the fatty acid oxidation studies and Z.T.S. and Z.G.-H. conducted the fatty acid oxidation assays. Z.T.S. and J.S.B. drafted the manuscript and all other authors made revisions.

Author Information

Reprints and permissions information is available at npg.nature.com/reprintsandpermissions.

normal matrix niches in the early stages of tumourigenesis when they proliferate into the lumen of hollow glandular structures. Filling of the luminal space is one of the hallmarks of early tumourigenesis.

Studies of luminal filling in both three-dimensional (3D) structures of MCF-10A mammary epithelial cells and the developing mammary gland have demonstrated that apoptosis is involved in clearance of centrally localised cells that lack matrix attachment; however, inhibition of apoptosis is not sufficient for survival of matrix-deprived cells in the luminal space[3,4,6,7]. Interestingly, several oncogenes, including ErbB2, have been shown to rescue cells from anoikis and prevent clearance of luminal cells in 3D acinar structures[8], suggesting that these oncogenes prevent luminal clearance programs in addition to anoikis.

Another striking feature of both matrix-detached MCF-10A cells and centrally located, matrix-deprived cells in MCF-10A acini is the induction of autophagy[9,10]. As autophagy is a catabolic process commonly upregulated under conditions of starvation[11], the association of this process with matrix deprivation suggests that ECM attachment regulates metabolic activity as well as apoptosis. Here we elucidate the basis for the metabolic defects in matrix-detached cells, demonstrate that oncogenes can rescue these defects through restoration of glucose uptake and enhancement of antioxidant capacity, and unexpectedly find that antioxidants alone can rescue matrix-detached cells via restoration of ATP generation through FAO. Lastly, we demonstrate that antioxidants promote anchorage-independent survival in two *in vitro* models of tumourigenesis.

To investigate whether ECM regulates cellular metabolism, we examined cellular ATP levels in MCF-10A cells cultured on adherent or non-adherent plates. We detected a substantial reduction in ATP in both MCF-10A (Fig. 1a) and primary human mammary epithelial cells (HMEC, Supplementary Fig. 2) that had been detached from the ECM for 24 hours. We confirmed these results in lysates normalized for total protein (Fig. 1b) and by measuring the ATP/ADP ratio (Fig. 1c). The reduction of ATP in MCF-10A cells occurred between 12 and 24 hours after ECM detachment (Supplementary Fig. 7), was not affected by inhibition of apoptosis (Fig. 1a and Supplementary Fig. 4,5) or autophagy (Supplementary Fig. 6), and was rescued by addition of reconstituted basement membrane (Supplementary Fig. 3). Expression of ErbB2 in these cells (ErbB2-MCF-10A) prevented the reduction in ATP following matrix detachment (Fig. 1a,c), suggesting that ErbB2 circumvents the matrix requirement for ATP production.

Given the evidence that EGFR is downregulated in detached cells and that its overexpression can rescue anoikis[12], we investigated the effect of ErbB2 on EGFR expression in detached cells. Indeed, ErbB2 expression caused a striking stabilization of EGFR following ECM detachment (Fig. 1d) that was critical for the rescue of ATP (Fig. 1e). This stabilization correlated with the maintenance of ERK activation and an enhancement of PI(3)K/Akt signaling (Fig. 1d); however, inhibition of PI(3)K (but not ERK) abrogated the ErbB2 rescue of ATP (Fig. 1f,g). Furthermore, expression of a constitutively active variant of PI(3)K (PIK3CA E545K) or Akt (Myr-Akt1) is sufficient to rescue detachment-induced ATP (Fig. 1h). These results indicate that ErbB2 rescues the metabolic defect in matrix detached cells by preventing the downregulation of EGFR andthus maintaining the activation of the PI(3)K pathway.

Given the critical role of PI(3)K/Akt in stimulating glucose transport13,14, we investigated whether glucose uptake is altered in matrix-detached cells. Indeed, we found a striking deficiency in glucose uptake in detached cells that was rescued (in a PI(3)K dependent fashion, Supplementary Fig. 8) by ErbB2 expression (Fig. 2a). In addition, treatment of detached cells with methyl pyruvate (MP), which provides substrates for the tricarboxylic acid (TCA) cycle,

causes a substantial increase in ATP (Fig. 2b) that is blocked by the mitochondrial Complex 1 inhibitor rotenone (Supplementary Fig. 9). This suggests that mitochondria of detached cells retain the capacity to produce ATP. To determine if the rescue of glucose uptake by ErbB2 is important for its ability to elevate ATP levels in detached cells, we treated ErbB2-MCF-10A cells with 2-deoxyglucose (2DG), a glucose analogue that inhibits glycolysis. 2DG treatment completely abolished the rescue of ATP by ErbB2 (Fig. 2c), confirming the importance of glucose uptake in the rescue of ATP by ErbB2.

Following cellular uptake, glucose can be further metabolised to generate ATP by glycolysis/oxidative phosphorylation, or it can be driven down the pentose phosphate pathway (PPP) by glucose-6-phosphate dehydrogenase (G6PDH)[15]. Since the PPP is a major source of cellular NADPH (which provides reducing equivalents), we examined the effects of matrix detachment on ROS production. ECM detachment induced a significant increase in ROS (Fig. 2d) and decrease in reduced glutathione (Fig. 2e), both of which were reversed by ErbB2 (Fig. 2d,f). In support of the possibility that the lack of PPP flux is responsible for the increase in ROS, we found that the reduction in glucose uptake precedes the elevation in ROS levels (Supplementary Fig. 10).

Previous studies have shown that reducing ROS through the stimulation of PPP flux can promote cell survival16,17; thus we hypothesised that PPP flux may be important for ErbB2 to rescue ATP levels in detached cells. Indeed, the treatment of detached ErbB2-MCF-10A cells with the PPP inhibitors dehydroisoandrosterone (DHEA) or 6-aminonicotinamide (6-AN) abrogated the ability of ErbB2 to rescue ATP (Fig. 2g) and led to an increase in cellular ROS (Supplementary Fig. 11). Interestingly, we found that matrix-detachment caused a significant increase in G6PDH protein (Fig. 2h), and siRNA-mediated reduction of G6PDH in detached ErbB2-MCF-10A cells caused a substantial decrease in ATP levels (Fig. 2i) and increase in ROS (Fig. 2j). The evidence that loss of matrix attachment causes an increase is ROS is consistent with studies in endothelial cells[18] and in the developing mammary gland[4].

The induction of ROS in suspended cells led us to investigate the effects of ROS neutralization on ATP in matrix-detached cells. Treatment of detached MCF-10A cells with the antioxidants N-acetyl-L-cysteine (NAC) or Trolox (a water-soluble Vitamin E derivative) significantly elevated ATP in detached cells (Fig. 3a) independent of any changes in glucose uptake (Fig. 3b). These data suggest that ROS inhibits ATP production through a metabolic pathway that could otherwise compensate for loss of glucose uptake.

It has previously been demonstrated that cancer cells deprived of glucose maintain ATP production through FAO[19]. Given that detached cells are glucose-deprived and antioxidants can promote ATP generation, we hypothesised that detachment-induced ROS could inhibit FAO. Indeed, we found that FAO was markedly reduced in detached MCF-10A cells (Fig. 3c) and Trolox treatment substantially elevated FAO (Fig. 3d). In addition, treatment of antioxidant-supplemented cells with etomoxir, an inhibitor of fatty acid transport into the mitochondria[19], prevented the rescue of ATP by antioxidants in detached cells (Fig. 3e). Furthermore, methyl malate treatment (which generates NADPH through an alternative pathway) elevated ATP levels, lowered ROS levels, and caused an increase in FAO in detached MCF-10A cells (Supplementary Fig. 12a–c) suggesting that NADPH production is sufficient to elevate FAO. Interestingly, ErbB2 reduced FAO in attached and suspended cells (Fig. 3c), consistent with previous reports showing PI(3)K/Akt mediated reduction of FAO[19,20]. However, treatment of detached ErbB2-MCF-10A cells with etomoxir caused a dose-dependent reduction in the ATP levels (Fig. 3f), suggesting that the residual FAO significantly contributes to ATP production in these cells.

To extend our analysis to a model with more physiologic relevance, we utilised the MCF-10A 3D cell culture model in which the inner, matrix-deprived cells show evidence of metabolic impairment (based on upregulation of autophagy9,10). While it is not feasible to measure ATP directly in these structures, we used two-photon microscopy to examine the native fluorescence of NADH and NADPH [NAD(P)H] and obtain an assessment of metabolic differences between the inner and outer cells21. Since NADH is the principal electron donor in glycolytic and oxidative metabolism, the native fluorescence of NAD(P)H represents a non-invasive fluorescent reporter of the metabolic state22. Images of acinar structures on Day 8 revealed a dichotomy in NAD(P)H fluorescence intensity between the inner and outer cells of the majority of structures, whereas most Day 4 structures showed homogenous fluorescence (Fig. 4a, Supplementary Fig. 13). Furthermore, we found that ROS were detectable exclusively in the centrally localized cells of Day 7 acini (Fig. 4c). Together, there results provide evidence that there are differences in metabolic activity and ROS accumulation in the matrix-deprived centrally localized cells of acini, as were observed in monolayer and suspension cultures (Figures 1–3). In addition, Trolox treatment prevented the dichotomy in NAD(P)H fluorescence in 3D culture (Fig. 4b, Supplementary Fig. 14), suggesting that ROS significantly contributes to the metabolic dichotomy between the inner and outer cells.

To understand the implications of these findings with regards to the clearance of cells from the luminal space, we studied the effects of antioxidant treatment on the survival of cells located in the center of acini. We treated acini with either NAC or Trolox and monitored luminal filling over time. Interestingly, we found that NAC or Trolox treatment significantly reduced luminal clearance (Fig. 4d) independent of effects on caspase activation (Supplementary Fig. 15), suggesting that the elimination of ROS can preserve the viability of matrix-deprived cells in the center of acini. By extrapolation to our studies showing ATP reduction and ROS generation in matrix-deprived cells, we speculate that the viability is a consequence of rescuing these metabolic impairments. In addition, the late clearing of acini observed in Bcl-2-MCF-10A cells is suppressed by Trolox. (Fig. 4d). These results suggest that suppression of both metabolic impairments and apoptosis are required for anchorage-independent survival.

The evidence that antioxidants can rescue metabolic defects of ECM-deprived cells and promote luminal filling in MCF-10A acini raises the question whether antioxidants could promote the transforming activity of mammary epithelial cells. To examine this, we assayed anchorage-independent colony formation in soft agar in MCF-10A cells expressing oncogenes that promote hyperproliferation (human papilloma virus E7 protein) and suppress apoptosis (Bcl-2). Neither E7 nor Bcl-2 expression rescued ATP in matrix detached cells (data not shown) and the E7/Bcl2 cells exhibited a relatively weak capacity to form colonies in this assay (Fig. 4e). Trolox treatment induced a substantial increase in the number and average size of colonies, suggesting that antioxidant treatment can enhance the transforming activity of cells that harbour oncogenic insults. We observed similar results with ErbB2-MCF-10A (Supplementary Fig. 16) and BT-474 cells, an ErbB2 expressing breast cancer cell line (Supplementary Fig. 17).

In summary, our study highlights the possibility that glucose deprivation could lead to ROS production during tumourigenesis and force selection for alterations that allow escape from oxidative damage. Furthermore, we demonstrate that antioxidants rescue cells from the need for glycolysis through stimulation of FAO. Thompson and coworkers[19] have previously shown that stimulation of FAO through AMPK/p53 is another mechanism for the survival of cells in the absence of glucose. Thus, our study suggests that deprivation of matrix may limit glucose accessibility during tumourigenesis, and reveals strategies whereby a tumour could escape from metabolic stress due to these conditions by stimulating anchorage-independent glucose transport and/or eliminating ROS.

In addition, these data demonstrate that antioxidants promote the survival of cells that lack attachment to the ECM and raise the question whether antioxidants may have dichotomous activities with respect to tumourigenesis -- that is, suppressing tumourigenesis by preventing oxidative damage to DNA23,[24], and promoting tumourigenesis by allowing survival of cells that are metabolically impaired (e.g. in altered matrix environments). In support of this, expression of SOD2, a mitochondrial protein that reduces oxidative stress caused by respiratory chain leak, is elevated in more advanced and higher grade mammary tumours[25],26. Furthermore, a recent study has revealed that enhanced PPP flux and increased antioxidant capacity correlates with metastasis of breast cancer cells to the brain27. Lastly, randomised trials have demonstrated both anti-neoplastic and neoplastic effects of antioxidants, with neoplastic effects associated with patients at higher risk due to smoking and alcohol consumption28, or patients undergoing chemo- or radiation therapy[29]. Our work provides a biological rationale for these findings, as antioxidant activity may promote the survival of pre-initiated tumour cells in unnatural matrix environments and thus enhance malignancy.

Methods Summary

MCF-10A cells and their variants were all cultured as described on http://brugge.med.harvard.edu/. Other cell lines were cultured as described in the supplementary information. All assays on ECM detached cells were carried out 24 hours after plating on poly-HEMA coated plates unless otherwise noted. ATP assays were conducted using either the ATPlite assay (PerkinElmer, Waltham, MA), the ATP determination kit (Invitrogen, Carlsbad, CA), or the ATP/ADP Ratio Assay Kit (BioAssay Systems, Hayward, CA). Glucose uptake assays were performed using the Amplex Red Glucose Assay Kit (Invitrogen). ROS was measured using carboxy-H_2DCF-DA in detached/attached cells and in 3D culture. To measure reduced glutathione, we used chloromethylcoumarin (CMAC, Invitrogen). FAO was measured by monitoring the release of $^{14}CO_2$ after addition of 1-^{14}C-Oleic Acid. 3D culture of mammary acini was completed according to the protocol at http://brugge.med.harvard.edu/. Native fluorescence of NAD(P)H was measured using two-photon microscopy. Soft agar assays were performed in the presence or absence of antioxidants and colony formation/size was determined using ImageJ.

Full methods and any associated references are available in the online version of the paper at www.nature.com/nature.

Supplementary Material

Refer to Web version on PubMed Central for supplementary material.

Acknowledgments

We thank Michael Overholtzer, Ghassan Mouneimne, Marco Mazzone, and Cheuk Leung for critical reading of the manuscript and/or experimental assistance. We thank Arnaud Mailleux, Alice Kaanta, Veronica Schafer, Alicia Zhou, Kaylene Simpson, and the members of the Brugge lab for experimental assistance, helpful comments, and/or discussion. This work was supported by a grant from the National Cancer Institute (J.S.B.) and a grant from the NIH (P.P.). Z.T.S. is the recipient of a Ruth L. Kirschstein National Research Service Award (NRSA) for Postdoctoral Fellows from the National Cancer Institute; L.S. an NCI Mentored Quantitative Research Development Award (K25); A.R.G. a National Science Graduate Research Fellowship; and H.Y.I. an NCI K08 Award.

References

1. Simpson CD, Anyiwe K, Schimmer AD. Anoikis resistance and tumor metastasis. Cancer Lett. 2008
2. Frisch SM, Screaton RA. Anoikis mechanisms. Curr Opin Cell Biol 2001;13:555–562. [PubMed: 11544023]

3. Debnath J, et al. The role of apoptosis in creating and maintaining luminal space within normal and oncogene-expressing mammary acini. Cell 2002;111:29–40. [PubMed: 12372298]
4. Mailleux AA, et al. BIM regulates apoptosis during mammary ductal morphogenesis, and its absence reveals alternative cell death mechanisms. Dev Cell 2007;12:221–234. [PubMed: 17276340]
5. Nelson CM, Bissell MJ. Of extracellular matrix, scaffolds, and signaling: tissue architecture regulates development, homeostasis, and cancer. Annu Rev Cell Dev Biol 2006;22:287–309. [PubMed: 16824016]
6. Debnath J, Brugge JS. Modelling glandular epithelial cancers in three-dimensional cultures. Nat Rev Cancer 2005;5:675–688. [PubMed: 16148884]
7. Humphreys RC, et al. Apoptosis in the terminal endbud of the murine mammary gland: a mechanism of ductal morphogenesis. Development 1996;122:4013–4022. [PubMed: 9012521]
8. Muthuswamy SK, et al. ErbB2, but not ErbB1, reinitiates proliferation and induces luminal repopulation in epithelial acini. Nat Cell Biol 2001;3:785–792. [PubMed: 11533657]
9. Fung C, et al. Induction of Autophagy during Extracellular Matrix Detachment Promotes Cell Survival. Mol Biol Cell 2008;19:797–806. [PubMed: 18094039]
10. Mills KR, et al. Tumor necrosis factor-related apoptosis-inducing ligand (TRAIL) is required for induction of autophagy during lumen formation in vitro. Proc Natl Acad Sci U S A 2004;101:3438–3443. [PubMed: 14993595]
11. Mathew R, Karantza-Wadsworth V, White E. Role of autophagy in cancer. Nat Rev Cancer 2007;7:961–967. [PubMed: 17972889]
12. Reginato MJ, et al. Integrins and EGFR coordinately regulate the pro-apoptotic protein Bim to prevent anoikis. Nat Cell Biol 2003;5:733–740. [PubMed: 12844146]
13. Czech MP, Corvera S. Signaling mechanisms that regulate glucose transport. J Biol Chem 1999;274:1865–1868. [PubMed: 9890935]
14. Elstrom RL, et al. Akt stimulates aerobic glycolysis in cancer cells. Cancer Res 2004;64:3892–3899. [PubMed: 15172999]
15. DeBerardinis RJ, Lum JJ, Hatzivassiliou G, Thompson CB. The biology of cancer: metabolic reprogramming fuels cell growth and proliferation. Cell Metab 2008;7:11–20. [PubMed: 18177721]
16. Bensaad K, et al. TIGAR, a p53-inducible regulator of glycolysis and apoptosis. Cell 2006;126:107–120. [PubMed: 16839880]
17. Boada J, et al. Cells overexpressing fructose-2,6-bisphosphatase showed enhanced pentose phosphate pathway flux and resistance to oxidative stress. FEBS Lett 2000;480:261–264. [PubMed: 11034341]
18. Li AE, et al. A role for reactive oxygen species in endothelial cell anoikis. Circ Res 1999;85:304–310. [PubMed: 10455058]
19. Buzzai M, et al. The glucose dependence of Akt-transformed cells can be reversed by pharmacologic activation of fatty acid beta-oxidation. Oncogene 2005;24:4165–4173. [PubMed: 15806154]
20. Deberardinis RJ, Lum JJ, Thompson CB. Phosphatidylinositol 3-kinase-dependent modulation of carnitine palmitoyltransferase 1A expression regulates lipid metabolism during hematopoietic cell growth. J Biol Chem 2006;281:37372–37380. [PubMed: 17030509]
21. Bennett BD, et al. Quantitative subcellular imaging of glucose metabolism within intact pancreatic islets. J Biol Chem 1996;271:3647–3651. [PubMed: 8631975]
22. Chance B, Cohen P, Jobsis F, Schoener B. Intracellular oxidation-reduction states in vivo. Science 1962;137:499–508. [PubMed: 13878016]
23. Gao P, et al. HIF-dependent antitumorigenic effect of antioxidants in vivo. Cancer Cell 2007;12:230–238. [PubMed: 17785204]
24. Narayanan BA. Chemopreventive agents alters global gene expression pattern: predicting their mode of action and targets. Curr Cancer Drug Targets 2006;6:711–727. [PubMed: 17168675]
25. Ivshina AV, et al. Genetic reclassification of histologic grade delineates new clinical subtypes of breast cancer. Cancer Res 2006;66:10292–10301. [PubMed: 17079448]
26. Sorlie T, et al. Gene expression patterns of breast carcinomas distinguish tumor subclasses with clinical implications. Proc Natl Acad Sci U S A 2001;98:10869–10874. [PubMed: 11553815]
27. Chen EI, et al. Adaptation of energy metabolism in breast cancer brain metastases. Cancer Res 2007;67:1472–1486. [PubMed: 17308085]

28. Omenn GS, et al. Effects of a combination of beta carotene and vitamin A on lung cancer and cardiovascular disease. N Engl J Med 1996;334:1150–1155. [PubMed: 8602180]

29. Lawenda BD, et al. Should supplemental antioxidant administration be avoided during chemotherapy and radiation therapy? J Natl Cancer Inst 2008;100:773–783. [PubMed: 18505970]

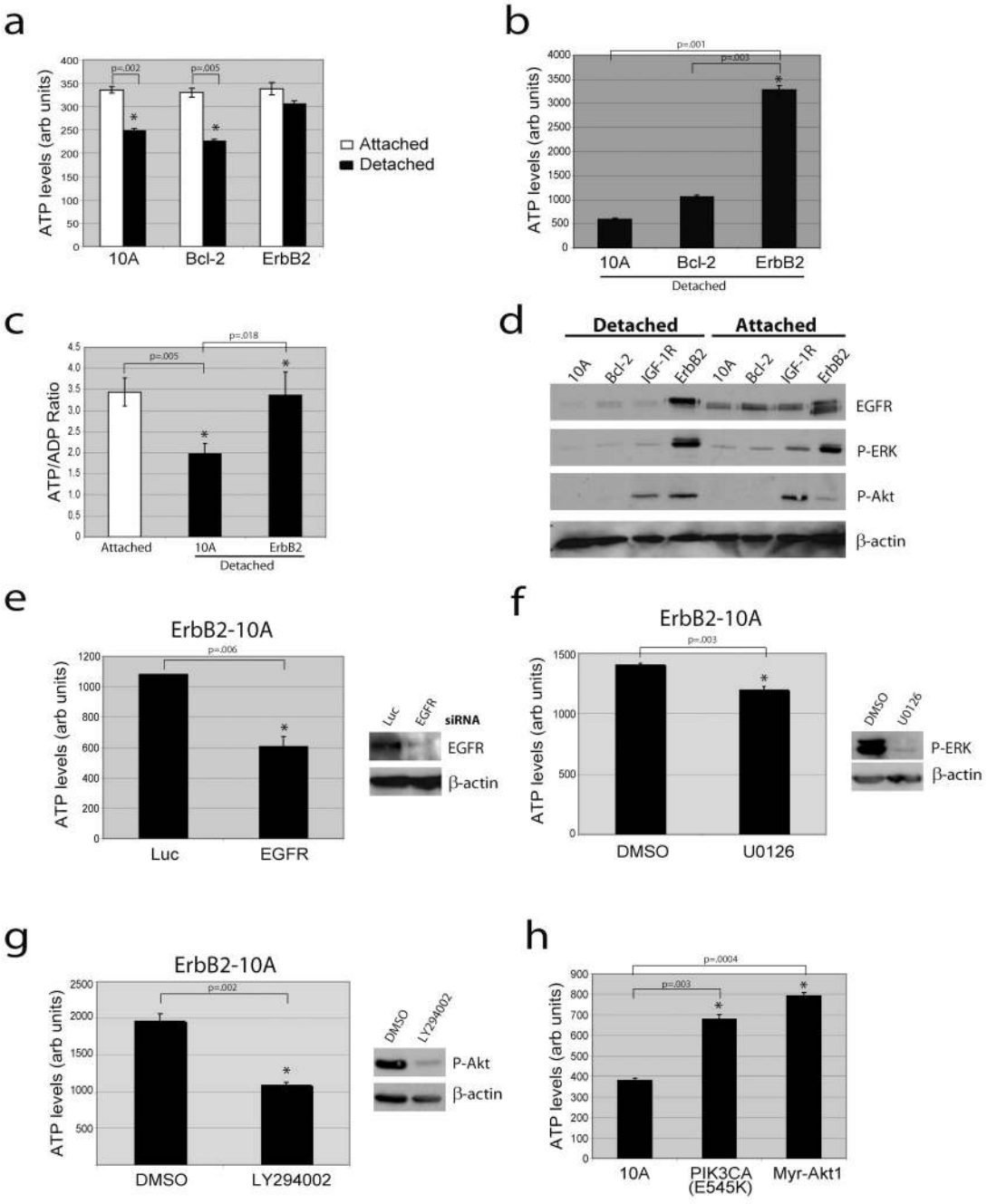

Figure 1. Loss of matrix attachment causes reduction in cellular ATP that is rescued by ErbB2 through PI(3)K pathway activation

(a) ATP was measured in the indicated cells 24 hours after plating in adherent or non-adherent (poly-HEMA-coated) plates using the ATPlite assay **(a)** or the ATP determination kit **(b).** **(c)** The ATP/ADP ratio was measured in the indicated cells. **(d)** The indicated cells were immunoblotted for EGFR, p-ERK, p-Akt, or β-actin. IGF-1R cells were used as a positive control for p-Akt. **(e)** ErbB2-MCF-10A cells were transfected with siRNAs targeting luciferase (luc) or EGFR and ATP levels were measured using the ATP determination kit. Knockdown was confirmed by immunoblot. **(f) and (g)** Detached ErbB2-MCF-10A cells were treated with 10 μM UO126 (ERK pathway inhibitor) **(f)** or 50 μM LY294002 (PI(3)K inhibitor) **(g)** for 24h

and ATP was measured using the ATP determination kit. Inhibition was confirmed by immunoblotting. **(h)** ATP was measured in detached 10A cells or 10A cells expressing PIK3CA (E545K) or Myr-Akt1 using the ATP determination kit. All error bars represent standard deviation (n=3). A * represents a statistically significant change calculated using a 2 tailed t test.

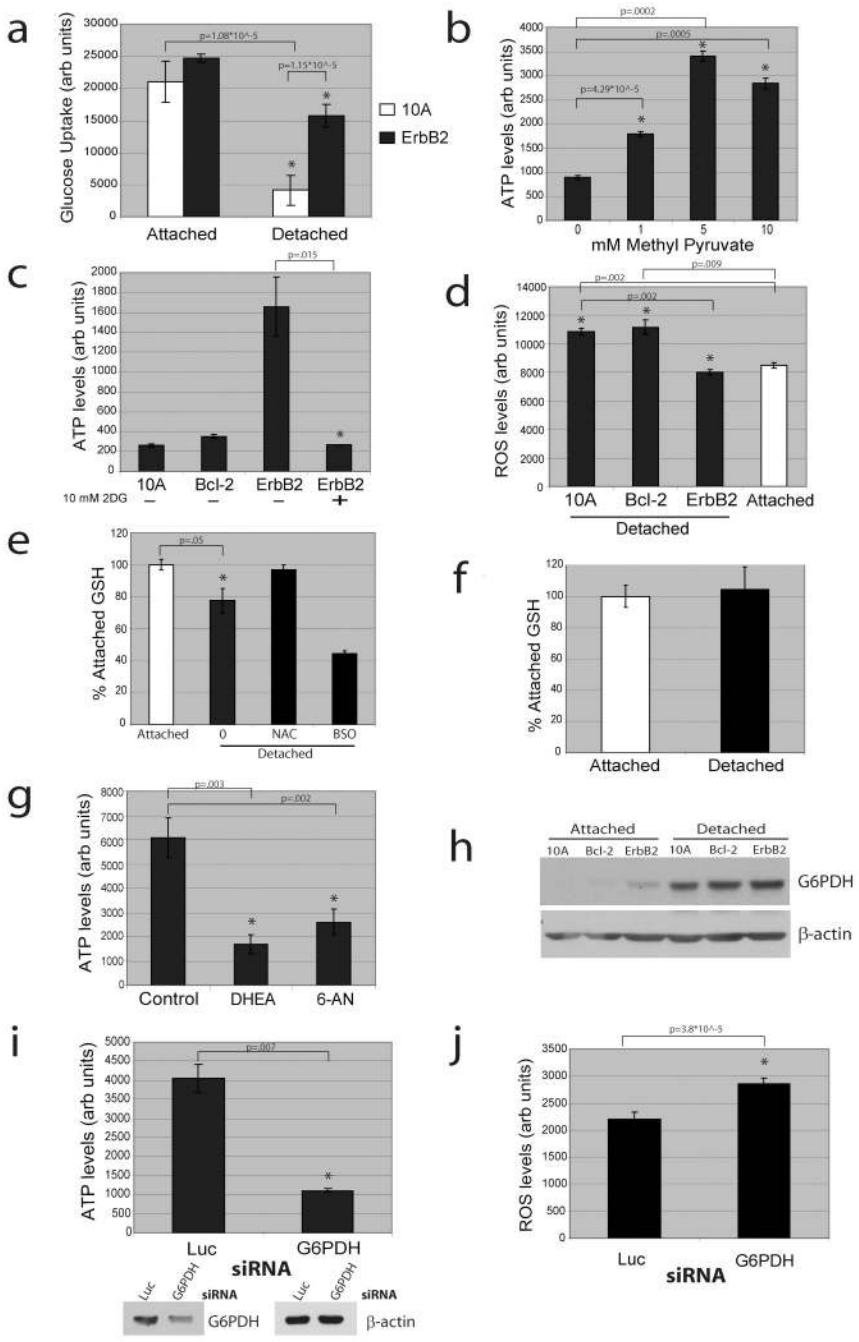

Figure 2. Matrix detachment causes a reduction in glucose uptake and ErbB2 rescue of this defect is dependent on PPP flux

(a) Glucose uptake was measured in the indicated cells using the Amplex Red assay. **(b)** ATP was measured using the ATP determination kit after treatment (where indicated) of detached cells with methyl pyruvate. **(c)** ATP was measured using the ATP determination kit after treatment (where indicated) of detached cells with 2DG. **(d)** ROS was measured in attached and detached cells using DCF-DA. **(e) and (f)** Reduced glutathione (GSH) was measured in 10A **(e)** or ErbB2-MCF-10A **(f)** cells. Results are graphed as the percent of the attached reduced GSH levels. 1 mM NAC and 1 mM BSO (an inhibitor of glutathione synthesis) were used as a positive and negative control. **(g)** ATP was measured using the ATP determination kit in

detached ErbB2-MCF-10A cells after treatment (where indicated) with vehicle control, 150 μM DHEA, or 150 μM 6-AN. **(h)** The indicated cell lines were immunoblotted for G6PDH after plating in either normal (attached) or poly-HEMA coated (detached) plates. **(i) and (j)** ATP **(i)** and ROS **(j)** were measured after siRNA mediated knockdown of G6PDH in detached ErbB2-MCF-10A cells. Knockdown was confirmed by immunoblotting. All error bars represent standard deviation (n=3). A * represents a statistically significant change calculated using a 2 tailed t test.

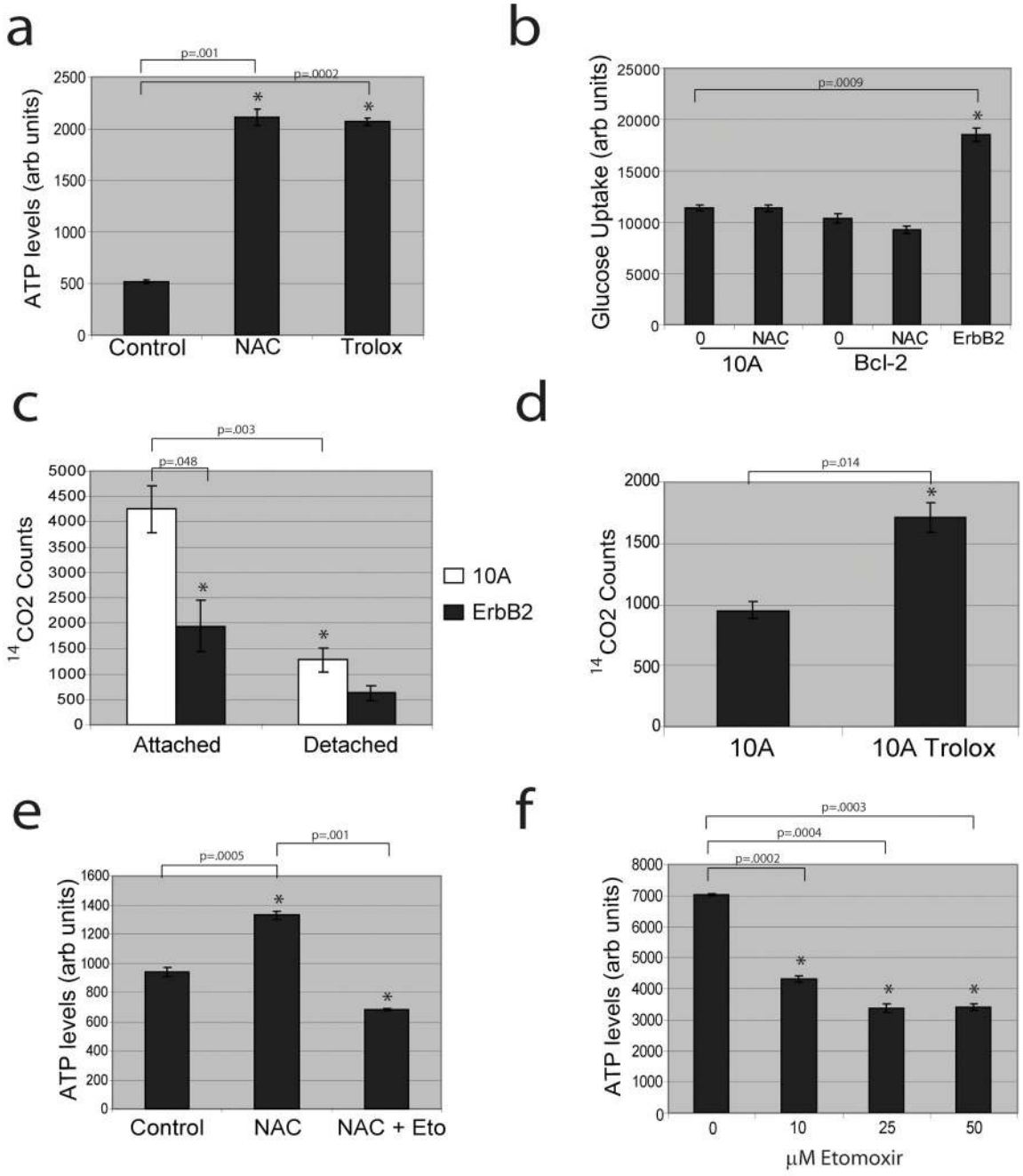

Figure 3. Antioxidants rescue low ATP levels in detached cells by permitting fatty acid oxidation

(a) MCF-10A cells were plated in poly-HEMA coated plates and treated with either control, 1 mM NAC, or 50 μM Trolox and ATP was measured using the ATP determination kit. **(b)** Detached 10A or Bcl-2-MCF-10A cells were treated with either vehicle (0) or 1 mM NAC and glucose uptake was compared to ErbB2-MCF-10A cells using Amplex Red assay. **(c)** FAO was measured in parental or ErbB2-MCF-10A cells (either attached or detached). **(d)** Detached MCF-10A cells were treated with either vehicle (10A) or 50 μM Trolox and FAO was measured. **(e)** Detached MCF-10A cells were treated with DMSO, 1 mM NAC, and/or 25 μM etomoxir and ATP was measured using the ATP determination kit. **(f)** Detached ErbB2-MCF-10A cells were treated with the indicated doses of etomoxir and ATP was measured using

the ATP determination kit. All error bars represent standard deviation (n=3). A * represents a statistically significant change calculated using a 2 tailed t test.

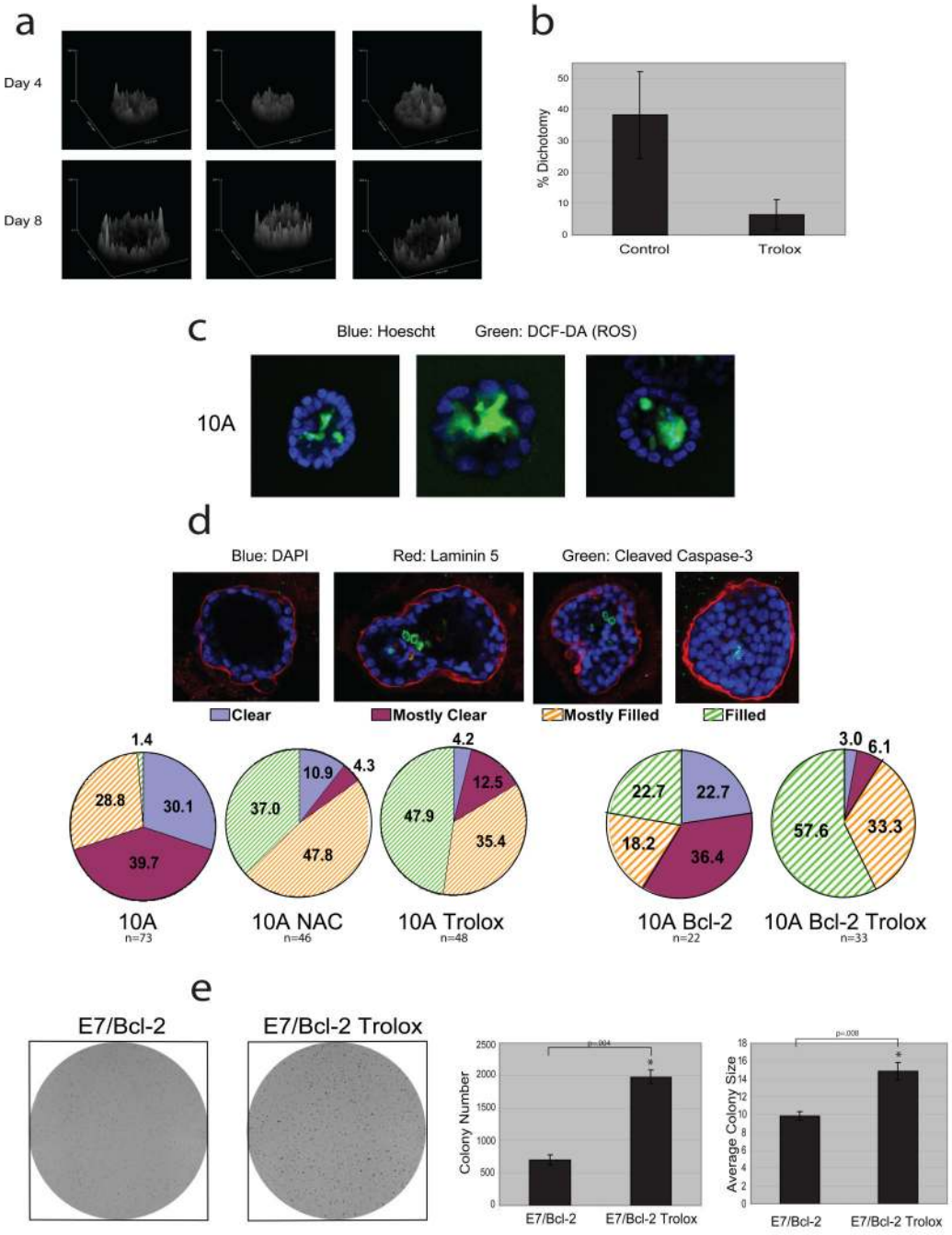

Figure 4. Analysis of antioxidant effects on acinar morphogenesis and colony formation in soft agar

(a) Native fluorescence of NAD(P)H was assayed by two-photon microscopy in MCF-10A acini. Surface intensity plots of three representative structures from Day 4 or Day 8 are shown. **(b)** Native fluorescence of NAD(P)H was assayed by two-photon microscopy in MCF-10A acini cultured in the presence or absence of 50 μM Trolox (added daily). At Day 8, structures were blindly scored for dichotomy in fluorescent intensity based on evidence of a reduction in fluorescence intensity in the inner cells (see examples in Supplementary Fig. 14). Error bars represent standard deviation of individual scorings (n=5). **(c)** ROS was measured in MCF-10A acini at Day 7, by staining with 25 μM DCF-DA (green) and Hoescht (blue). Three representative images are shown and 41% (n=73) of all structures were positive for DCF-DA

staining exclusively in the inner cells. NAC or Trolox treatment inhibited the DCF-DA staining in acini (data not shown). **(d)** Acini were formed using 10A or Bcl-2-MCF-10A cells (10A or 10A Bcl-2) and treated with 1 mM NAC or 50 μM Trolox where indicated. At Day 19 (10A) or Day 33 (Bcl-2), acini were stained for laminin 5, cleaved caspase-3, and with DAPI. Acini were then scored as described. **(e)** 10A cells expressing E7 and Bcl-2 were plated in soft agar and after 20 days, images were taken after INT-violet staining. Colony number and average colony size were determined using ImageJ. Error bars represent standard deviation (n=3 unless otherwise indicated). A * represents a statistically significant change calculated using a 2 tailed t test.